3   Witold M. Lewandowski*
4   Michał Ryms
5   Hubert Denda
6
7   Faculty of Chemistry, Department of Chemical Apparatus and Theory of Machines, Gdansk
8   University of Technology, ul. G. Narutowicza 11/12, 80-233 Gdansk, Poland
9   *wlew@pg.gda.pl

10   **Keywords**
11   natural convection, infrared imaging, convectors, exchangers, vertical symmetrically heated
12   plates

13   **Abstract**

14   The study describes natural convection through a vertical channel, open on four sides and bound by
15   two isothermal walls. Both balancing and infrared experimental investigations were performed in air
16   (Pr = 0.71) to estimate the impact of channel width s and wall-to-ambient temperature difference (t_w -
17   t_∞) on natural convective heat transfer, the formation of air flow patterns and the rate of flow pattern
18   formation. The study was conducted on two parallel vertical plates of height H = 0.5 m and width B =
19   0.25 m, with the heated surfaces facing each other, thus creating peripherally open channels of
20   different widths s = 0.045, 0.08, 0.180 and ∞ m. The surface temperature t_w, identical for both heating
21   plates, was changed every 10 K and set at t_w = 40, 50, 60, 70 and 80 °C, while the ambient temperature
22   was maintained within the 18 to 25 °C range. In the balance method, heat fluxes were determined
23   based on measurements of voltage and electric current supplying the heaters placed inside the walls. In
24   the gradient method, the heat fluxes were calculated from the temperature distribution in air, within a
25   plane perpendicular to the heating plate surfaces. Temperature fields were visualized using a plastic
26   detecting mesh and a thermal imaging camera. The distribution of temperature $t_{x,y}$, and its gradient at
27   the walls $\mathrm{d}t/\mathrm{d}x|_{x=0,y}$ were obtained at different heights y along the channels. The gradient values
28   obtained and the results, presented as dependencies of the Nusselt number on the Rayleigh number,
29   indicate that the channel width has a significant impact on heat transfer. Compared to the vertical plate
30   $s = \infty$, the following levels of convective heat transfer intensification were observed: 29.5% (s = 0.045
31   m), 38.8% (s = 0.085 m) and 61.6% (s = 0.180 m).

32

33   **1. Introduction**

34   The research resulting in this study was inspired by questions which arose during the
35   construction of convector plate air heaters, illustrated in Fig.1.
36

37   **Figure 1**

38
39   The most important of these questions is whether increasing the width of the plate
40   spacing intensifies or inhibits convective heat transfer and what the optimal spacing of these
41   plates should be. Prior to exploring this problem, it was necessary to locate it within the map
42   of multiple convective heat exchange cases. These include convective heat transfer in an open
43   space, taking place from flat (vertical, diagonal, horizontal) [1],[2],[3], cylindrical (horizontal,
44   diagonal, vertical) [4],[5],[6], spherical and complex surfaces [7],[8],[9]. An equally
45   important issue is natural convection in a closed space, occurring inside cylindrical, spherical
46   or cuboid ducts [10]. In the latter case, the ambient thermodynamic conditions neither
47   intensify nor inhibit the phenomena occurring inside the channels. However, if these channels
48   are open on one side (top, bottom, front or rear), on two sides (rear and front or top and
49   bottom) or on all four sides, there is an indirect case of natural convection, formally occurring
50   in a closed space but simultaneously inhibiting or intensifying the impact of the environment.
51   Despite its many practical applications, e.g. in construction (convector heaters, air
52   heaters, coolers) or electronics (heatsinks, components and electronic components), this case

has not been tested very often, as evidenced by the next section of this study, which analyzes papers on convective heat exchange in channels.

2. Literature review

In order not to duplicate previously published results, but rather utilize this research creatively to further the development of science, it must be preceded by a thorough study of the literature. The results of such a study concerning natural convection in vertical, flat channels are given below and summarized in Table 1.

Depending on the configuration of the boards and their temperature in convective heat transfer in channels, the following cases can be specified [11], [12]:

- natural convection in a vertical, closed space, known as Rayleigh-Bénard convection [13], [14], [15], [16], [17], [18],

- convection in a vertical, partially heated [19] or open channel (at the top/bottom or on all sides) [20], [21], [22],

- convection in a vertical gap for the following conditions:

    - symmetric: isoflux [23], [24], [25] or isothermal heating plates [23], [24], [26], [27], [28], [29]

    - asymmetric (hot-cold, hot-adiabatic, warm-hot) isoflux [30], [31], [23], [24], [32], [19] or isothermal heating plates [33], [34], [35], [36], [37], [38], [31], [23], [24], [39], [40], [41], [42],

- vertical plane with an open-ended channel and isothermal, symmetrically heated walls [43], [44], [31],

- vertical plane channel with different wall temperatures (hot-cold, hot-adiabatic, warm-hot) [38], [45], [46]

Any of these configurations can be investigated theoretically (analytically: [31], [23], [47], numerically: [17], [21], [37], [43], [44], [48], [48], [46], [51], [52], [53], [53], [55], [19], [40], [41], [37], [56], [57],), experimentally: [17], [20], [35], [20], [39], [44], [58], [59], [60], [53], [61], [41], [37] or tested by visual methods [62], [64], [64],[18], [65].

The context of this division is presented on the diagram of a plate convective air heater (radiator, Fig.1). The current work focuses on the experimental and visual study of natural convection within such a device, formed by two vertical, parallel, isothermal, symmetrically heated channels open on four sides. The criteria for the Nusselt and Rayleigh numbers are listed in Table 1.

Table 1

3. The test stand

The research stand (Fig. 2) utilized in tests of convective heat transfer between two parallel surfaces, with different distances *s* between them, consisted of two identical, vertically mounted, parallel plates with their heating surfaces facing each other. A detection grid was fixed between the plates, perpendicular to their heating surfaces and parallel to the force of gravity, enabling temperature to be detected with a thermal imaging camera.

Figure 2

Each plate was constructed from three 495 mm by 247 mm aluminum sheets of different thicknesses. The 12-mm thick outer sheet was the plate's heating surface. The two inner sheets (center and rear) were 10 mm thick. Two flat heaters (main and auxiliary) were attached to the outer aluminum sheets. The main heater (300W) was used for heating the plate. The 150W auxiliary heater, located at the rear of the plate, compensated the backflow of heat from the main heater to the plate. Two textolite laminate sheets (6 mm thick) were installed between the aluminum sheets, serving as a thermal and electrical insulator. With this

1 setup, the external aluminum surface was precisely heated and its isothermicity maintained at
2 the set temperature. The construction diagram of a single plate is shown in Figure 3.
3
4 **Figure 3**

5   32 thermocouples were installed in the experimental stand. Each hotplate was fitted
6 with 12 of these thermocouples, while the remaining 8 were placed in the surroundings of the
7 plates, within the area of undisturbed heat flow. Based on data provided by the
8 thermocouples, the following temperatures were measured for each simulation board:
9   - the temperature of the vertical surface of the heated plate t_w, which was the average
10 of the readings of 4 thermocouples placed on the external aluminum sheet of the main heater;
11   - the temperature of the central aluminum plate on the main heater side t_m, which was
12 the average of the 4 thermocouple readings;
13   - the temperature of the aluminum back plate on the secondary heater side, which was
14 the average of the 4 thermocouple readings.
15   The test stand was equipped with a computer-controlled, automatic control system,
16 which maintained the set temperature of the heating surface t_w by controlling the current-
17 voltage characteristics, thus adjusting the main and auxiliary heater power $N = U \cdot I$ in such a
18 way that the temperature difference between both sides of the laminate remained zero $\Delta t = t_m$
19 $- t_a = 0$. For a relatively small plate thickness and $\Delta t = 0$, it can be assumed that the total
20 heating power from both heated surfaces is converted into a heat flux, according to the
21 relationship $Q = N_I + N_{II} = U_I \cdot I_I + U_{II} \cdot I_{II}$, and then transferred by convection to the air inside
22 the channel between two vertical plates. To minimize radiation emissions, the aluminum
23 surfaces of both plates were polished.
24   A single heating plate test to confirm the possibility of measuring a convective heat
25 flux in air with thermal imaging, including theoretical fundamentals and test procedures, is
26 described in detail in [68] and [69]. In this study, the same method of measuring a heat flux
27 was utilized for the open gaps between plates, encountered in devices such as convectors
28 (Fig.1).
29

30 **4. Description of the measurement methodology**
31 The sensitivity range of the thermal imaging camera covers wavelengths from about 1 to 15
32 μm. However, for natural convection within the temperature range $0 < t < 100$ ºC, air does not
33 emit radiation in this wavelength range. Therefore, to ensure proper temperature
34 measurement, an intermediary element in the form of a mesh was utilized as a radiation
35 detector. The mesh was fixed in such way that the grid was parallel to the convective heat flux
36 and perpendicular to the heating surface (Fig.2).
37   The fibers of the mesh, flushed by the convective free-flow forming in the channel,
38 heated to the ambient air temperature, allow the temperature field within the channel to be
39 detected with a thermal imaging camera. The mesh has a sufficiently low thermal
40 conductivity and a fiber diameter small enough to prevent temperature equalization on the
41 grid surface. At the same time, it has a sufficiently high thermal inertia for conducting
42 accurate measurements. Moreover, the small fiber dimensions do not inhibit the air flow.
43 During the tests, a cotton mesh with a fiber diameter of $d = 0.4$ mm and mesh size of $a = 1.6$
44 mm was impregnated with polyester material to achieve a thermal conductivity of $\lambda = 0.02$
45 W/(m·K). This material was selected based on preliminary visualizations of temperature fields
46 in vertical slots during convective heat transfer [70] using an IR-FlexCam® Fluke Ti35.
47   When selecting the distance between the plates, the relationship derived by Bar-Cohen
48 et al. [23] (Table 1) for the same case of two isothermal, symmetrically heated vertical panels,
49 forming a channel open on four sides, was utilized:
50
51     $s_{opt} = 2.714 \, (Ra/H)^{-0.25}$,   (1)
52

3

from which, for given Rayleigh numbers within the laminar range $Ra = 10^4$, 10^5 and 10^6, as well as for the plate height of $H = 0.5$ m, the following results were obtained:

$$s = 0.137 \text{ m } (Ra = 10^4) \, , \quad s = 0.076 \text{ m } (Ra = 10^5) \text{ and } \quad s = 0.043 \text{ m } (Ra = 10^6) \, . \quad (2)$$

Because prior to the experiment the variation range of the Rayleigh number was unknown, it was decided to adopt approximations of the calculated values of $s = 0.045$, 0.085 and 0.180 m. Meshes of a suitable width were prepared, stretched over a frame, stiffened with a polyester lacquer and placed perpendicularly to the surface of the heating plates at half their width $z = 0.5$ **B**.

The study was conducted using two vertical plates of height $H = 0.5$ m and width $B = 0.25$ m, the heating surfaces being arranged parallel to each other. Thus, vertical planes with circumferential openings and spacings $s = 0.045$, 0.085 and 0.180 m were formed.

The surface temperature of each heating plate t_w was adjusted by 10 K within the range of $40 \leq t_w \leq 80$ °C, while the ambient temperature was kept within $18 \leq t \leq 25$ °C. The temperature field in the channel was measured in the plane perpendicular to the heated surfaces, in the center of the plates' width $z = 0.5$ **B**. Previous studies showed that the z coordinate had no significant effect on the results. The temperature fields in the three cross-section layers $z = 0.0$, $z = 0.25$ **B** and $z = 0.5$ **B** are qualitatively convergent [68], [69], [70]. Therefore, the study was limited to the coordinate $z = 0.5$ **B**, which was considered representative of the whole channel.

All the tests described in this paper were conducted using a FlexCam® Fluke Ti35 IR camera with total accuracy of $\Delta T = 0.1$ K. The device was set up at a constant distance of 2 m from the grid, perpendicular to the grid and parallel to the heating surface.

5. Results of temperature field and temperature gradient investigations

Selected results obtained on the test stand, schematically illustrated in Fig. 2, are shown in Figures 4-7. The temperature fields in the cross-sectional plane between the two vertical isothermal plates **I** and **II** were respectively determined for $s = 0.045$ m, $s = 0.085$ m and $s = 0.18$ m.

Figures 4-7

The plots in Figures 4-6 are limited to five temperatures t_w, characteristic of convector operation. Full channel study results have already been published [70]. In addition, Figure 7 shows previously unpublished temperature fields for two parallel, vertical plates fixed at such a distance that their convective fluxes do not interact with each other. This case, treated as a reference point, is denoted as $s = \infty$.

The digital values of the channel temperature distributions ($s = 0.045$, 0.085, 0.180 and ∞ m) between plates **I** and **II** in the plane (x, y), at different heights y, constant mesh setting, and at half the width of the plates ($z = 0.5$ **B**), obtained for variable plate surface temperatures $t_w = 40$, 50, 60, 70 and 80 °C, are summarized in Table 2.

Table 2

Examples of temperature profiles observed at level $y = 0.5$ **H** but only for $s = \infty$ are illustrated graphically in Figure 8. The temperature profile for the other case of $s = 0.045$, 0.085 and 0.180 m have already been published in [70].

Figure 8

1   The temperature gradients $\mathrm{d}t/\mathrm{d}x|_{x=0}$ on both sides of heating plates **I** and **II**, for $s =\infty$,
2 are calculated from equation (3), based on the data collected in table 2.

3
$$\left.\frac{\partial t}{\partial x}\right]_{x=0,\mathrm{I}} = \frac{(t_0=t_\mathrm{w})-t_1}{x_1-(x_0=0)} \ \ (\textbf{I}) \ \text{ and } \ \left.\frac{\partial t}{\partial x}\right]_{x=0,\mathrm{II}} = \frac{(t_n=t_\mathrm{w})-t_{n-1}}{(x_n=s)-x_{n-1}} \ \ (\textbf{II}). \tag{3}$$

4   The results of these calculations for temperatures $40 \le t_\mathrm{w} \le 70$ °C at different channel
5 heights $0 \le y \le H$ and for a constant width $z = 0.5\,B$ are listed in Table 3, but only for $s = \infty$.
6 Similar results have already been published for the other channels $s = 0.045$, 0.085 and 0.180
7 m [70].
8
9 <div align="center">**Table 3**</div>

10 **6. Results of the balance method analysis**

11 The results of the balance method of the experiments are presented in the first column of
12 Table 4 in the form of $C_\mathrm{b}=Nu_\mathrm{b}/(Ra_\mathrm{b})^{1/4}$ relations, obtained for the test channels by averaging
13 the values for the two plates **I** and **II**, according to the procedure described in [68], [69] and
14 [70]. However, the differences between them are so small ($\pm 1.7\%$ from the mean value) that it
15 is not possible on their basis to indicate which gap will be the most advantageous in the heat
16 exchanger. It was therefore decided to validate these results using the gradient method. Aside
17 from enabling local values to be determined, this method also allows the mechanisms of
18 convective heat transfer to be investigated depending on channel width.

19 **7. Results of the gradient method analysis**

20 Assuming that heat transfer from isothermal vertical flat surfaces to the air inside a single
21 channel is two-dimensional, the local heat fluxes in a steady state, at level y, in the x direction,
22 are described by the Fourier and Newton formulae:

23
$$-\lambda \cdot A \cdot \left.\frac{\partial t}{\partial x}\right]_{x=0,y} = h_y \cdot A \cdot \left(t_\mathrm{w} - t_{\infty,y}\right) \ \text{ and then } \ h_y = \lambda \cdot \frac{-\frac{\partial t}{\partial x}\big]_{x=0,y}}{t_\mathrm{w}-t_{\infty,y}}, \tag{4}$$

24 where t_w, °C – temperature of the wall at level y, $t_{\infty,y}$, °C – lowest air temperature inside the
25 channel at level y, h, W/(m²K) – heat transfer coefficient, and λ, W/(m·K) – thermal
26 conductivity of air.
27   The local heat transfer coefficients $\alpha_\mathrm{y,I}$ and α_yII, obtained from equation (4) for both
28 surfaces of vertical plates **I** and **II** as a function of temperature t_w and level y for different
29 channel widths ($s = 0.045$, 0.085, 0,180 m and ∞), can be calculated according to the
30 relationship (5) into averages for whole **I** and **II** surfaces, as well as for whole channels (6):

31
$$\overline{h_\mathrm{I/II}} = \frac{1}{H}\int_0^H h_{y,\mathrm{I/II}}dy = \frac{\lambda}{H}\int_0^H \frac{-\frac{\partial t}{\partial x}\big]_{x=0,y}}{t_\mathrm{w}-t_{\infty,y}}\,dy, \tag{5}$$

32
$$h = \frac{\overline{h_\mathrm{I}}+\overline{h_\mathrm{II}}}{2}. \tag{6}$$

33   The calculated local heat transfer coefficients $h_\mathrm{y,I}$ and $h_\mathrm{y,II}$ along y for plates **I** and **II,**
34 creating channels of width $s = 0.045$, 0.085 and 0.180 m, as well as their averaged values (5)
35 and (6), are presented graphically in [70].
36   In the gradient method, convective heat transfer can also be presented using the
37 averaged Nusselt number Nu_y according to the formula:

38
$$Nu = \frac{1}{H}\int_0^H Nu_y dy = \frac{1}{H}\int_0^H \frac{h_y}{\lambda}\cdot y \cdot dy = \frac{1}{H}\int_0^H \frac{-\frac{\partial t}{\partial x}\big]_{x=0,y}}{t_\mathrm{w}-t_\infty}\cdot y \cdot dy. \tag{7}$$

The Nusselt - Rayleigh relationship describing the experimental results obtained using the gradient method are defined as:

$$Nu = C \cdot Ra^{1/4} \ , \tag{8}$$

in which the Nusselt Nu and Rayleigh Ra numbers are defined as:

$$Nu = \frac{h \cdot H}{\lambda} \quad \text{and} \quad Ra = \frac{g \cdot \beta \cdot (t_w - t_\infty) H^3}{a \cdot \nu} \ , \tag{9}$$

where H, m – height of the heated plates (the characteristic linear dimension), g, m/s^2 – acceleration due to gravity, β, 1/K – coefficient of cubic expansion and a, ν, m^2/s – thermal diffusivity and kinematic viscosity.

The physical properties of air (a, β, ν and λ) were determined for a mean air temperature t_{av} using the formula $t_{av} = (t_{w,I} + t_{w,II} + 2t_{\infty,y})/4$, taking into account the surface temperatures of both plates t_{wI} and t_{wII} measured with thermocouples, as well as the lowest air temperature $t_{\infty,y}$ in the channel at level y. In the case of two vertical heating plates which, due to the large distance $s = \infty$ did not thermodynamically interact with each other, the surface temperature was additionally measured with a thermal imaging camera. If $t_{w,I} = t_{w,II}$ and $t_{\infty,I} = t_{\infty,II}$, the average air temperature t_{av} can be defined traditionally as $t_{av} = (t_{w,I} + t_{w,II})/2$. Additionally, to prevent accidental air movement caused by ventilation or drafts, the tests were carried out in an insulated room.

The results of convective heat transfer for the channels, calculated from equation (8) in the form of the Nusselt and Rayleigh numbers (non-averaged) shown graphically in Figure 9, are also listed in the second column of Table 4 in the form of $C=Nu/(Ra)^{1/4}$.

Figure 9

Table 4

The discrepancies between the balance and gradient methods (Table 4), which can be compared due to the same characteristic linear dimension H, are reproducible and are equal to $52 \pm 7\%$. They are caused by differences in defining the Nusselt numbers Nu_b and Nu. In case of the balance method, local values are not averaged, whereas in the gradient method this is required for local heat transfer coefficients $h_{y,I}$ and h_{yII} or for $Nu_{y,I}$ and $Nu_{y,II}$ along y. In addition, radiation has different effects in both cases. In the balance method, the combined convection and radiation heat flux is measured, while in the gradient method, the radiation flux is only marginally detected by the mesh placed parallel to the direction of the radiation. Furthermore, in the case of smaller channels, the radiation flux is trapped inside these channels and also heats up the mesh. However, a more thorough study of these phenomena would require further research not directly related to the present work.

The results listed in the first two columns of Table 4 indicate that the intensity of convective heat transfer is a function of the distance s between the plates. The effect, however, is more evident than in the case of the balance method. In practice, therefore, the gradient method utilizing a thermal imaging camera is more useful for qualitative heat transfer studies in channels than the balance method. In this case, the intensification of convective heat exchange in relation to $s = \infty$ was observed for all channels and was equal to 33.9% ($s = 0.045$ m), 13.8% ($s = 0.085$ m) and 31.3% ($s = 0.180$ m).

The results obtained by the gradient method, presented in Table 4, were developed based on the dependence of $Nu = C \, Ra^{1/4}$, in which H is a characteristic linear dimension (8). However, the height of all the channels was the same ($H = 0.5$ m), in contrast to the width, which was variable $s = 0.045$, 0.085, 0.180 and 0.250.

Therefore, it was decided to evaluate the influence of channel width s on the results, presenting them in the form of the dependence (10):

$$Nu^* = C^* \cdot Ra^{*\,1/4} \ , \tag{10}$$

6

in which the Nusselt and Rayleigh numbers are now defined as:

$$Nu^* = \frac{h \cdot s}{\lambda} \quad \text{and} \quad Ra^* = \frac{g \cdot \beta \cdot (t_w - t_\infty)s^3}{a \cdot v} \; , \tag{11}$$

For this purpose, the following conversion factor was used:

$$C^* = \frac{Nu}{Ra^{1/4}}\left(\frac{s}{H}\right)^{1/4} \qquad C^* = C\left(\frac{s}{H}\right)^{1/4} \tag{12}$$

The results, obtained using the gradient method and recalculated on the basis of dependence (12) are as follows:

$$Nu^* = 1.094\,(0.045/0.5)^{1/4}\,Ra^{*\ 1/4} = 0.599 \cdot Ra^{*\ 1/4} \text{ for } s = 0.045 \text{ m}, \tag{13}$$

$$Nu^* = 0.945\,(0.085/0.5)^{1/4}\,Ra^{*\ 1/4} = 0.607 \cdot Ra^{*\ 1/4} \text{ for } s = 0.085 \text{ m}, \tag{14}$$

$$Nu^* = 1.073\,(0.180/0.5)^{1/4}\,Ra^{*\ 1/4} = 0.831 \cdot Ra^{*\ 1/4} \text{ for } s = 0.180 \text{ m}, \tag{15}$$

$$Nu^* = 0.817\,(0.250/0.5)^{1/4}\,Ra^{*\ 1/4} = 0.826 \cdot Ra^{*\ 1/4} \text{ for } s = \infty \, , \tag{16}$$

It was assumed that from $s/H > 0.5$, the channel concept becomes meaningless and we are now dealing with two independent vertical plates. In equation (16) we therefore assumed that $s = 0.5\,H = 0.250$ m.

The averaged value of the above dependences ((13) – (16)) is

$$Nu^* = 0.716 \cdot Ra^{*\ 1/4} \pm 0.11 \; . \tag{17}$$

Unfortunately, the analysis of all the results listed in Table 4, regardless of the methods of acquiring or converting them, still does not give a definite answer to the question as to what the optimal distance between the plates of the heat exchanger under consideration should be. In this situation, it was decided to present the results directly in the form of local temperature gradient dependences $\overline{dt/dx}|_{x=0,y,\mathrm{I,II}} = f\,(y,s,t_w)$, omitting local heat transfer coefficients $h_{y,\mathrm{I,II}}$, as shown in Fig.10.

Figure 10

In addition to local temperature gradients, the averaged results for plates **I**, **II** and for the whole channel are illustrated in this figure.

8. Discussion

The results, illustrated in Fig. 10 as correlations of average temperature gradients, show the impact of channel width s on the intensity of convective heat flux more clearly than previous results, expressed as mean heat penetration coefficients α or Nusselt Nu numbers.

The dependences of temperature gradients $dt/dx|_{x=0,\mathrm{tot}}$, averaged for y and t_w, on channel width s presented in Fig.11, are directly related to the heat flux transmitted to the air according to the equation:

$$q = q_\mathrm{I} + q_\mathrm{II} = -\lambda \cdot \overline{\frac{\partial t}{\partial x}}\Bigg]_{x=0,tot} \tag{18}$$

Assuming that, after averaging, the thermal conductivity of air λ is the same for the entire temperature range investigated, the impact of channel width on the intensification of the heat transfer in the channel, in relation to $s = \infty$, is 29.5% ($s = 0.045$ m), 38.8 % ($s = 0.085$ m) and 61.6% ($s = 0.180$ m).

Figure 11

7

Further research is required to explain the reasons for this intensification of heat exchange. However, even at this stage of the study, which is confirmed by the visualization of the temperature fields in the channels, the convective air fluxes and the air flow patterns created by them can be described by the following mechanisms:

$s \approx 0$ - due to the insufficiently high values of Nusselt and Rayleigh numbers, heat transfer occurs only through conduction, which is low in air,

$s\uparrow$ - after exceeding the critical Rayleigh number, convective heat transfer begins, which is more intense than conduction; however, inhibiting interactions between the plate walls suppress the flux and heat exchange,

$s\uparrow\uparrow$ - a chimney effect is created, which is no longer suppressed by the presence of the walls, and the intensity of the convective heat transfer reaches a maximum,

$s\uparrow\uparrow\uparrow$ - a further increase in the distance between the plates disrupts the chimney effect, as the heated air flows out of the channel through the sides, which begin to inhibit heat transfer,

$s\uparrow\uparrow\uparrow\uparrow$ - the chimney effect disappears, but the streams flowing next to each other generate turbulence, which keeps the heat exchange at a lower yet still high level.

$s \rightarrow \infty$ - the two convective fluxes no longer interact, and the intensity of convective heat transfer is the same as for a typical, single, vertical plate.

The three s values tested in this paper have confirmed their utility, according to equation (1), and the results can be creatively used in the design of convective air heaters with vertical plates. However, a closer examination of convective flow patterns, as well as the ranges in which the particular channel mechanisms occur, requires further research with a larger number of channels.

9. Conclusions

This paper analyses free convective heat transfer within air channels between two vertical, parallel, isothermal and symmetrically heated plates, investigated using the gradient method with a thermal imaging camera. This research topic and configuration of convective heat exchange were inspired by convector-type air heaters, which have a similar construction, with the aim of using the results of these studies to optimize such devices. It was once again confirmed that the gradient method utilizing a thermal imaging camera can be applied to complex convective heat transfer studies performed on the basis of previous work in this field [68], [69] and [70].

The results presented as temperature fields $t(x,y)$ and temperature gradient distributions $\partial t/\partial x \big|_{x=0,y}$, can provide a basis for describing and interpreting the convective heat transfer phenomenon in vertical plate channels open on four sides.

References:

[1] A. Mitsuishi, A. Sakai, K. Kitamura i T. Misumi, „Fluid Flow and Heat Transfer of Mixed Convection Adjacent to Vertical Heated Plates Placed in Uniform Horizontal Flow of Air, Heat Transfer—Asian Research, 38(6) (2009) 347-360.

[2] H. Denda, W.M. Lewandowski, M. Ryms, P.Wcisło, Attempts of Thermal Imaging Camera Usage in Estimations of the Convective Heat Loss From a Vertical Plate, EUROTHERM Seminar 101 "Transport Phenomena in Multiphase Systems", Kraków (2014) 1-6.

[3] H. Denda, W.M. Lewandowski, M. Ryms, Określanie konwekcyjnych strat ciepła z pionowych powierzchni budynków za pomocą nowej metody, Rynek Instalacyjny, 9 (2015) 34-40.

[4] S. Acharya, S.K. Dash, Natural Convection Heat Transfer from a Short or Long, Solid or Hollow Horizontal Cylinder Suspended in Air or Placed on Ground, Journal of Heat Transfer, 139(7) (2017), Article number 072501.

[5] M. Ali, Experimental free convection heat transfer from inclined square cylinders, Heat and Mass Transfer/Waerme- und Stoffuebertragunge, 53 (2017) 1643-1655.

[6] D. Subramanyam, Experimental analysis of natural convection over a vertical cylinder, International Journal of Applied Engineering Research, 10 (2015) 44326-44329.

[7] Z. Brodnianska, J. Cernecky,The impact of the shaped vertical heated surfaces on the values of the heat transfer coefficients, JP Journal of Heat and Mass Transfer, 13 (2016) 575-588.

[8] W.M. Lewandowski, E. Radziemska, Heat transfer by free convection from an isothermal vertical round plate in unlimited space, Applied Energy, 68 (2001) 187-201.

[9] W.M. Lewandowski; S. Szymanski, P. Kubski et al. Natural convective heat transfer from isothermal conic, International Journal of Heat And Mass Transfer, 42 (1999) 1895-1907.

[10] E. Radziemska, W.M. Lewandowski, Experimental verification of natural convective heat transfer phenomenon from isothermal cuboids. Experimental Thermal And Fluid Science, 32 (2008) 1034-1038.

[11] A. Baïri, E. Zarco-Pernia, J.M. García de María, A review on natural convection in enclosures for engineering applications. The particular case of the parallelogrammic diode cavity, Applied Thermal Engineering, 63 (2014) 304-322.

[12] A-J.N. Khalifa, Natural convective heat transfer coefficient - a review II. Surfaces in two- and three-dimensional enclosures, Energy Conversion and Management, 42 (2001) 505-517.

[13] M. Nansteel, R. Greif, Natural convection in undivided and partially divided rectangular enclosures, Journal of Heat Transfer, 103 (1981) 623-629.

[14] J.K. Platten, J.C. Legros, Convection in Liquids, part.C, Springer-Verlag, 1983.

[15] H.K. Wee, Heat and Mass Transfer in confined spaces, PhD thesis, University of Canterbury, 1986.

[16] F. Penot, A. Ndame, Successive bifurcations of natural convection in vertical enclosure heated from the side, 1st European Thermal Sciences, vol. 1, Birmingham, UK, 1992, pp. 507–514.

[17] A. Baïri, N. Laraqi, J.M. García de María, Numerical and experimental study of natural convection in tilted parallelepipedic cavities for large Rayleigh numbers, Experimental Thermal and Fluid Science, 31 (2007) 309–324.

[18] E.R.G. Eckert, W.O. Carlson, Natural Convection in an Air Layer Enclosed Between Two Vertical Plates with Different Temperatures, International Journal of Heat and Mass Transfer, 2 (1961) 106-120.

[19] S. Taieb, L.A. Hatem, J. Balti, Natural convection in an asymmetrically heated vertical channel with an adiabatic auxiliary plate, International Journal of Thermal Sciences, 74 (2013) 24-36.

[20] E.M. Sparrow, P.A. Bahrami, Experiments on Natural Convection from Vertical Parallel Plates with Either Open or Closed Edges, J. Heat Transfer, 102(2) (1980) 221-227.

[21] A.G. Fedorov, R. Viskanta, Turbulent natural convection heat transfer in an asymmetrically heated, vertical parallel-plate channel, International Journal of Heat Mass Transfer, 40 (16) (1997) 3849-3860.

[22] N.A.A. Qasem, B. Imteyaz, R. Ben-Mansour, M. A. Habib, Effect of Radiation Heat Transfer on Naturally Driven Flow Through Parallel-Plate Vertical Channel, Arabian Journal for Science and Engineering, 42 (2017) 1817–1829.

[23] A. Bar-Cohen, W.M. Rohsenow, Thermally Optimum Spacing of Vertical, Natural Convection Cooled, Parallel Plates, ASME Journal of Heat Transfer, 106(1) (1984) 116-124.

[24] A. Bar-Cohen, H. Schweitzer, Convective immersion cooling of parallel vertical plates. Hybrids, and Manufacturing Technology, IEEE Transactions 8(3) (1985) 343-351.

[25] T. Inagaki, S. Maruyama, Turbulent Heat Transfer of Natural Convection Between Two Vertical Parallel Plates, Heat Transfer – Asian Research, 31(1) (2002) 56-67.

[26] A-J.N. Khalifa, Natural convective heat transfer coefficient - a review II. Surfaces in two- and three-dimensional enclosures, Energy Conversion and Management, 42 (2001) 505-517

[27] G. Desrayaud, E. Chenier et al., Benchmark solutions for natural convection flows in vertical channels submitted to different open boundary conditions, International Journal of Thermal Sciences, Elsevier, 72 (2013) 18-33

[28] S.W. Churchill, R. Usagi, A General Expression for the Correlation of Rates of Transfer and Other Phenomena, AIChE Journal, 18(6) (1972) 1121-1128.

[29] Reda I. El-Ghnam, Numerical Investigation of Natural Convection Heat Transfer between Two Vertical Plates with Symmetric Heating, International Journal of Thermal Technologies, Vol.5, No.1 (2015), s. 31-44

[30] A.L. Pica, G. Rodno, R. Volpes, An experimental investigation on natural convection of air in a vertical channel, International Journal of Heat and Mass Transfer, 50 (2007) 2612–2623.

[31] W. Elenbass, Heat dissipation of parallel plates by free convection, Physica, 9 (1942) 1–28.

[32] O. Miyatake, T. Fujii, M. Fujii, H. Tanaka, Natural Convective Heat Transfer Between Vertical Parallel Plates – One Plate with a Uniform Heat Flux and the other Thermally Insulated, Heat Transfer – Japanese Research, 4 (1973) 25-33.

[33] P. Kiš, H. Herwig, Natural convection in a vertical plane channel: DNS results for high Grashof numbers, Heat Mass Transfer, Springer-Verlag Berlin Heidelberg 50(7) (2014) 957–972. DOI 10.1007/s00231-014-1305-5.

[34] A.G. Fedorov, R. Viskanta, Turbulent natural convection heat transfer in an asymmetrically heated, vertical parallel-plate channel, International Journal of Heat Mass Transfer, 40 (16) (1997) 3849-3860.

[35] M.A. Habib, S.A.M. Said, S.A. Ahmed, A. Asghar, Velocity characteristics of turbulent natural convection in symmetrically and asymmetrically heated vertical channels, Experimental Thermal and Fluid Science, 26 (2002) 77–87.

[36] F.J. Higuera, Yu.S. Ryazantsev, Natural convection flow due to a heat source in a vertical channel, International Journal of Heat and Mass Transfer, 45 (2002) 2207–2212.

[37] T.Yilmaz, S.M.Fraser, Turbulent natural convection in a vertical parallel-plate channel with asymmetric heating, International Journal of Heat and Mass Transfer, 50 (2007) 2612–2623.

[38] E.M. Sparrow, L.F.A. Azevedo, Vertical channel natural convection spanning between the fully developed limit and single plate boundary layer limit, International Journal of Heat and Mass Transfer, 28 (1985) 1847–1857.

[39] O. Miyatake, T. Fujii, Free Convective Heat Transfer Between Vertical Plates – One Plate Isothermally Heated and the Other Thermally Insulated, Heat Transfer – Japanese Research, 3 (1972) 30-38.

[40] V.I. Terekhov, A.L. Ekaid, Laminar Natural Convection between Vertical Isothermal Heated Plates with Different Temperatures, Journal of Engineering Thermophysics, 20(4) (2011) 416–433.

[41] A.S. Krishnan, B. Premachandran, C. Balaji, S.P. Venkateshan, Combined experimental and numerical approaches to multi-mode heat transfer between vertical parallel plates, Experimental Thermal and Fluid Science, 29 (2004) 75–86.

[42] S-C.Wong, S-H. Chu, Revisit on natural convection from vertical isothermal plate arrays--effects of extra plume buoyancy, International Journal of Thermal Sciences 120 (2017) 263-272.

[43] A. Andreozzi, B. Buonomo, O. Manca, Transient Natural Convection in Vertical Channels Symmetrically Heated at Uniform Heat Flux, Numerical Heat Transfer, Part A: Applications: An International Journal of Computation and Methodology, 55 (2009) 409-431.

[44] Z. Amine, C. Daverat, S. Xin, S. Giroux-Julien, H. Pabiou, C. Ménézo, Natural Convection in a Vertical Open-Ended Channel: Comparison between Experimental and Numerical Results, Journal of Energy and Power Engineering 7 (2013) 1265-1276.

[45] W. Aung, L.S. Fletcher, V. Sernas, Developing laminar free convection between vertical plates and asymmetric heating, International Journal of Heat and Mass Transfer, 16 (1972) 2293–2308.

[46] H.M. Salih, Numerical Simulation for Laminar Natural Convection with in a Vertical Heated Channel, Eng. & Tech. Journal, 29(11) (2011), 2298-2311.

[47] N. Srivastava, A.K. Singh, Mixed convection in a composite system bounded by vertical walls, Journal of Applied Fluid Mechanics, 3(2) (2010) 65-75.

[48] S.J. Ormiston, A numerical study of two-dimensional natural convection in a Trombe wall system including vent and room effects. M.A.Sc.Thesis, Dept. of Mechanical Engineering, University of Waterloo (December 1983).

[49] L. Martin, G.D. Raithby, M.M. Yovanovich, On the Law Rayleigh Number Asymptote for Natural Convection Through an Isothermal, Parallel-Plate Channel, ASME Journal of Heat Transfer, 113 (1991) 899-905

[50] J.R. Bodia, J.F. Osteral, The development of free convection between heated vertical plates ASME J. Heat Transfer, 84 (1962) 40–44.

[51]. N.A.A.Qasem, B.Imtryaz, R.Ben-Mansour, M.A.Habib, Effect of Radiation Heat Transfer on Naturally Driven Flow Through Parallel-Plate Vertical Channel, Arab. J. Sci. Eng., Published online 17 October 2016, DOI 10.1007/s13369-016-2319-8.

[52] T. Inagaki, K. Komori, Numerical modeling on turbulent transport with combined forced and natural convection between two vertical parallel plates, Int. J. Comput. Meth. A 27 (4) (1995) 417–431.

[53] D. Ospir, C. Chereches, C. Popa, S. Fohanno, C. Popovici, Flow dynamics in a double-skin façade, Proceedings of the 3rd WSEAS International Conference on Finite Differences – Finite Elements – Finite Volumes – Boundary Elements (2009).

[54] A. Mokni, H. Mhiri , G. Le Palec, Ph. Bournot, Mixed convection in a vertical heated channel: influence of the aspect ratio, International Journal of Engineering and Applied Sciences 5(1) (2009) 60-66.

[55] K.M. Çakar, Numerical investigation of natural convection from vertical plate fined heat sinks, M.Sc. Thesis submitted to The Middle East Technical University (2009).

[56] B. Rama Bhupal Reddy, A numerical study on developed laminar mixed convection with vertical channel in downflow, International Journal of Physical and Social Sciences, 2(3) (2012) 72-88.

[57] W.Aung, G. Worku, Developing flow and flow reversal in a vertical channel with asymmetric wall temperatures, ASME Journal of Heat Transfer 108 (1986) 299–304.

[58] A.L. Pica, G. Rodono, R. Volpes, An experimental investigation of free convection heat transfer in vertical channels with backward facing step, ASME, Fluids Eng.Div. 238 (3) (1993) 263–270.

[59] A. Daloglu, T. Ayhan, Natural convection in a periodically finned vertical channel, Int.Commun. Heat Mass Transfer 26 (8) (1999) 1175–1182.

[60] S.C. Lin, K.P. Chang, Y.H. Hung, Natural convection within a vertical finite-length channel in free space, J.Thermophys. Heat Transfer 8 (2) (1994) 366–368.

[61] Q. Lu, S. Qiu, G. Su., W. Tian, Z. Ye, Experimental research on heat transfer of natural convection in vertical rectangular channels with large aspect ratio, Experimental Thermal and Fluid Science 34 (2010) 73–80.

[62] J.L. Wright H. Jin, K.G.T. Hollands, D. Naylor, Flow visualization of natural convection in a tall, air-filled vertical cavity, International Journal of Heat and Mass Transfer 49(5) (2006) 889-904.

[63] Z.Y. Guo, Y.Z. Song, X.W. Zhao, Experimental Investigation on Natural Convection in Channel by Laser Speckle Photography, Experimental Thermal and Fluid Science, 4 (1991) 594-600.

[64] K. Kato et al. Heat Transfer in a Channel between Vertical Electronic Circuit Boards Cooled by Natural Air Convection, Journal of Chemical Engineering of Japan 24(5) (1991) 568-574.

[65] G. Polidori, S. Fatnassi, R. Ben Maad, F. Beaumont, S. Fohanno, Transient natural convection flow dynamics in a asymmetrically heated vertical channel, 10th International Conference on Heat Transfer, Fluid Mechanics and Thermodynamics 14–16 July 2014.

[66] G.D. Raithby, K.G.T. Holland, A general method of obtaining approximate solution to laminar and turbulent free convective problems. Advanced Heat Transfer, 11 (1975) 266-315.

[67] G.D. Raithby, K.G.T. Holland, Natural convection, W.M. Rosenhow, J.P. Hartnett, E.N. Ganic (Eds.), Handbook of Heat Transfer Fundamentals (second ed.), McGraw-Hill, New York (1985) (Chapter 6)

[68] W.M. Lewandowski, M. Ryms, H. Denda, E. Klugmann-Radziemska, Possibility of thermal imaging use in studies of natural convection heat transfer on the example of an isothermal vertical plate, International Journal of Heat and Mass Transfer, 78 (2014) 1232-1242.

[69] W.M. Lewandowski, H. Denda, M. Ryms, E. Klugmann-Radziemska, Method for measuring flow of heat in solid-gas system, involves determining low heat transfer coefficient of infrared radiation detector, and determining alternating field temperature of IR detector by using thermal imager. Patent PL412090-A1.

[70] W.M.Lewandowski, M. Ryms, H. Denda, Infrared techniques for natural convection investigations in channels between two vertical, parallel, isothermal and symmetrically heated plates, International Journal of Heat and Mass Transfer, 114 (2017) 958-969.

List of figures

Fig.1 Diagram of a multi-plate convector with natural convective temperature and velocity fields, generated in air between two adjacent plates.

List of tables

Nomenclature

a = thermal diffusivity, m²/s

b = half-width of channel, $\equiv s/2$, m

A = area, $\equiv 2HB$, m²; coefficient

B = plate width, m

C = coefficient

1   g = acceleration due to gravity, m/s^2

2   h = heat transfer coefficient, W/(m^2 K)

3   H = channel or vertical plate length, m

4   I = amperage of electric current, A

5   m = exponent in Eqs. (2) and (5)

6   Nu = Nusselt number, $\equiv \alpha H/\lambda$ dimensionless (9)

7   Nu_b = channel balance Nusselt number, $\equiv UI/(\lambda(t_w\text{-}t_\infty)B)$ dimensionless

8    $\widetilde{Nu}$ = modified Nusselt number, $\equiv UIs/(\lambda(t_w\text{-}t_\infty)H^2)$ dimensionless

9   Nu_y = local Nusselt number, $\equiv \alpha y/\lambda$ dimensionless

10   Nu = total Nusselt number, dimensionless

11   Nu^*= total channel Nusselt number, $\equiv \alpha s/\lambda$, dimensionless (10)

12   P = plate/air parameter, $\equiv Ra/H^4$, m^{-4}

13   q'' = heat flux, $\equiv q/A$, W/m^2

14   Ra = Rayleigh number, $\equiv g\beta\Delta tH^3/(\nu a)$, dimensionless (9)

15   Ra^* = channel Rayleigh number, $\equiv g\beta\Delta ts^3/(\nu a)$, dimensionless (10)

16    $\widetilde{Ra}$ = modified Rayleigh number, $\equiv g\beta\Delta tb^3/(\nu a)\cdot H/b$, dimensionless

17   s = plate spacing, m

18   t = temperature, ^{o}C

19   T = temperature, K

20   U = voltage of electric current, V

21   x,y,z= coordinates, m

22

Greek Letters

24   β = volumetric coefficient of thermal expansion, 1/K

25   λ = thermal conductivity, W/(m K)

26   ν = kinematic viscosity, m^2/s

27   ρ = density, kg/m^3

28   ∞ = entrance or ambient value

29

Subscripts

31   a   = auxiliary

32   av   = average,

33   b   = balance method

34   m   = main,

35   w   = wall,

36   y   = local

37
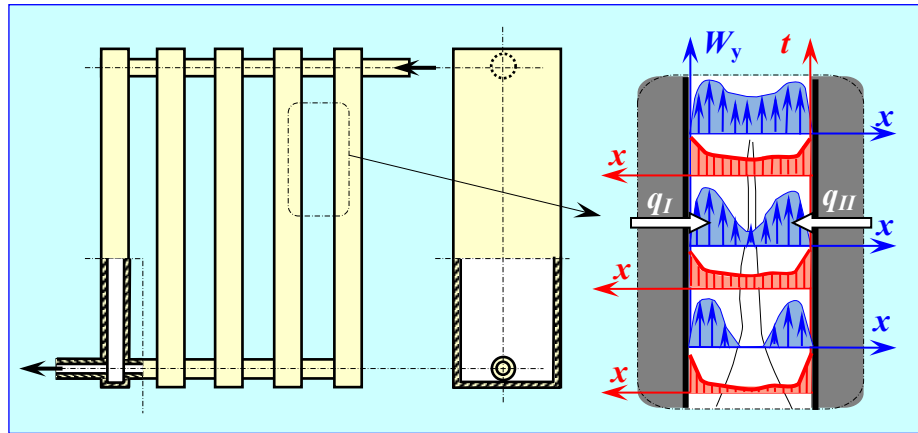
Figure 1
Schematic of a multi-plate convector with natural convective temperature and velocity fields, generated in air between two adjacent plates.
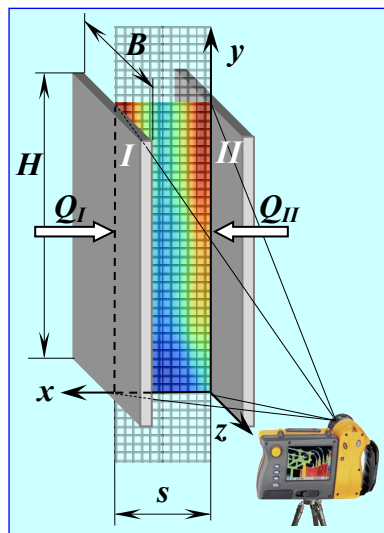
Figure 2
Diagram of the experimental setup consisting of two isothermal, vertical plates and a mesh allowing the detection of temperature field in the air with a thermal imaging camera.
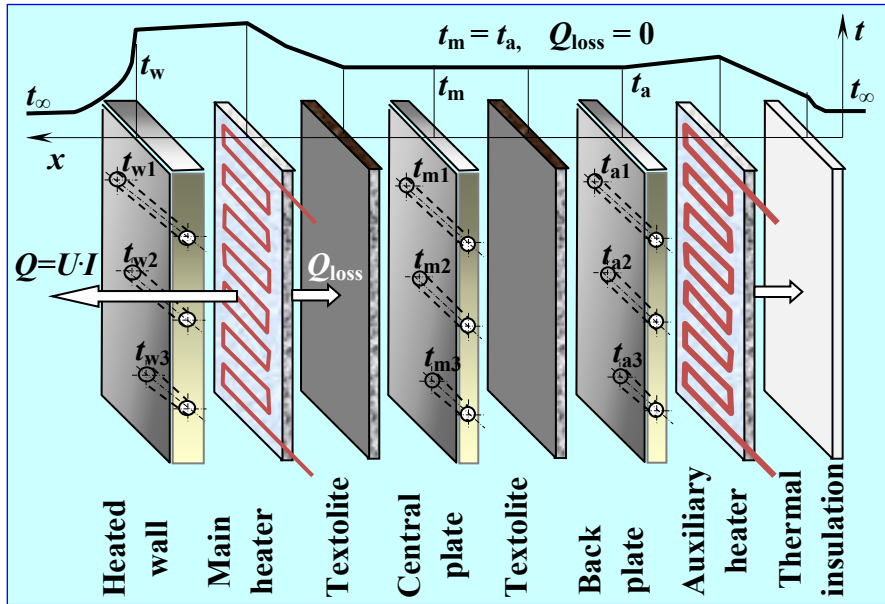
Figure 3

Construction diagram for two identical, vertical heating plates utilized in the study of convective heat transfer in open channels
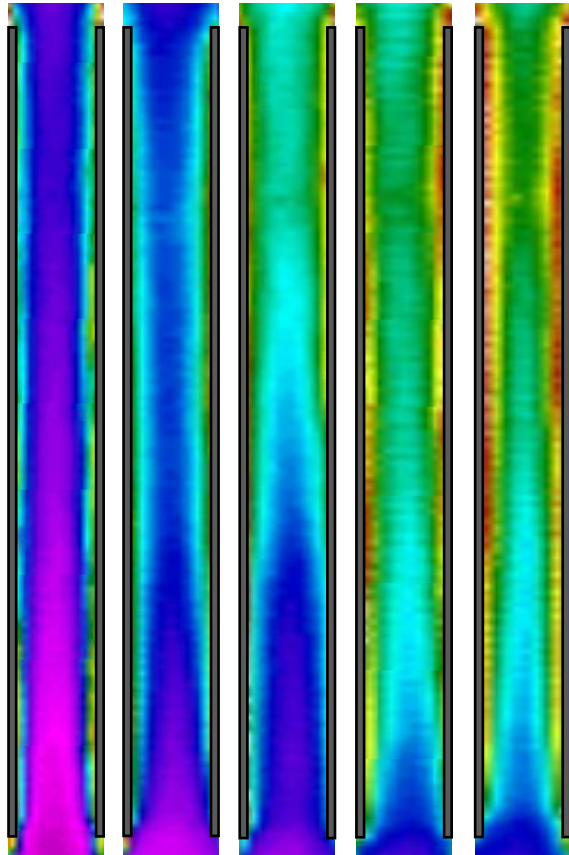
Figure 4
Temperature fields in the channel *s* = 0.045 m between the vertical isothermal heated plates as a function of their surface temperature t_w and the ambient temperature t_∞ in the *x*, *y*, *z*= 0.5 *B* planes.
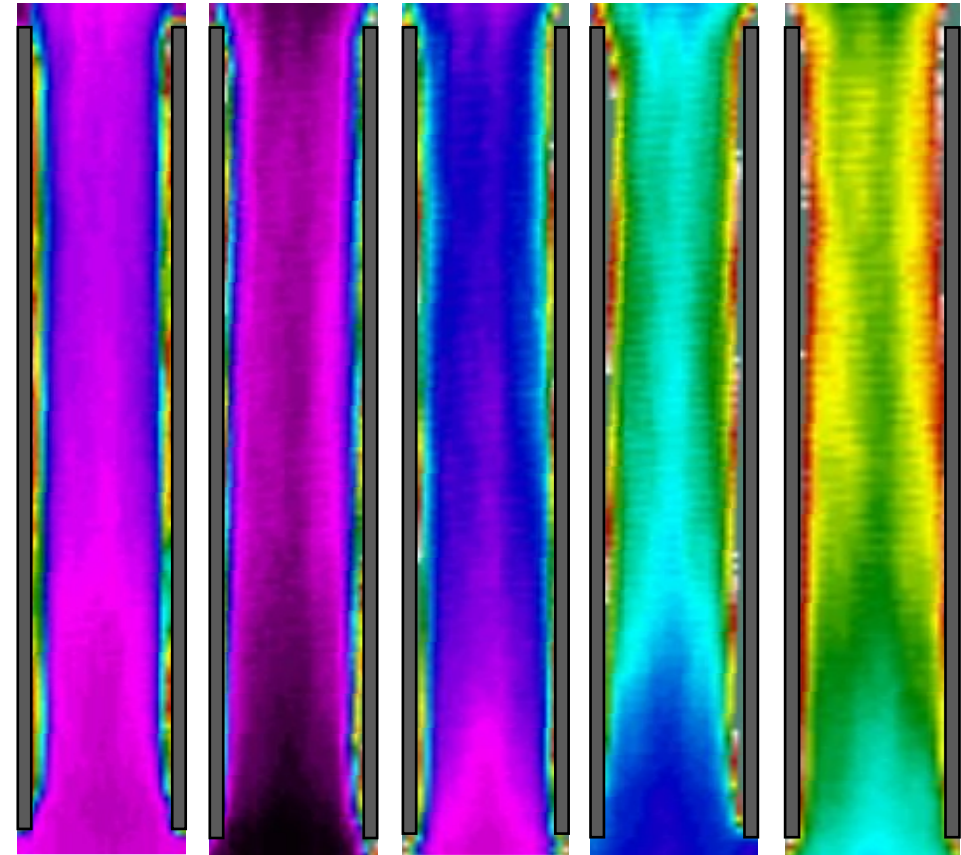
Figure 5
Temperature fields in the channel *s* = 0.085 m between the vertical isothermal heated plates as a function of their surface temperature t_w and the ambient temperature t_∞ in the *x*, *y*, *z*= 0.5 *B* planes.

25.0　25.5　26.0　26.5　27.0　27.5　28.0　28.5　29.0　29.5　30.0　30.5　31.0 ºC
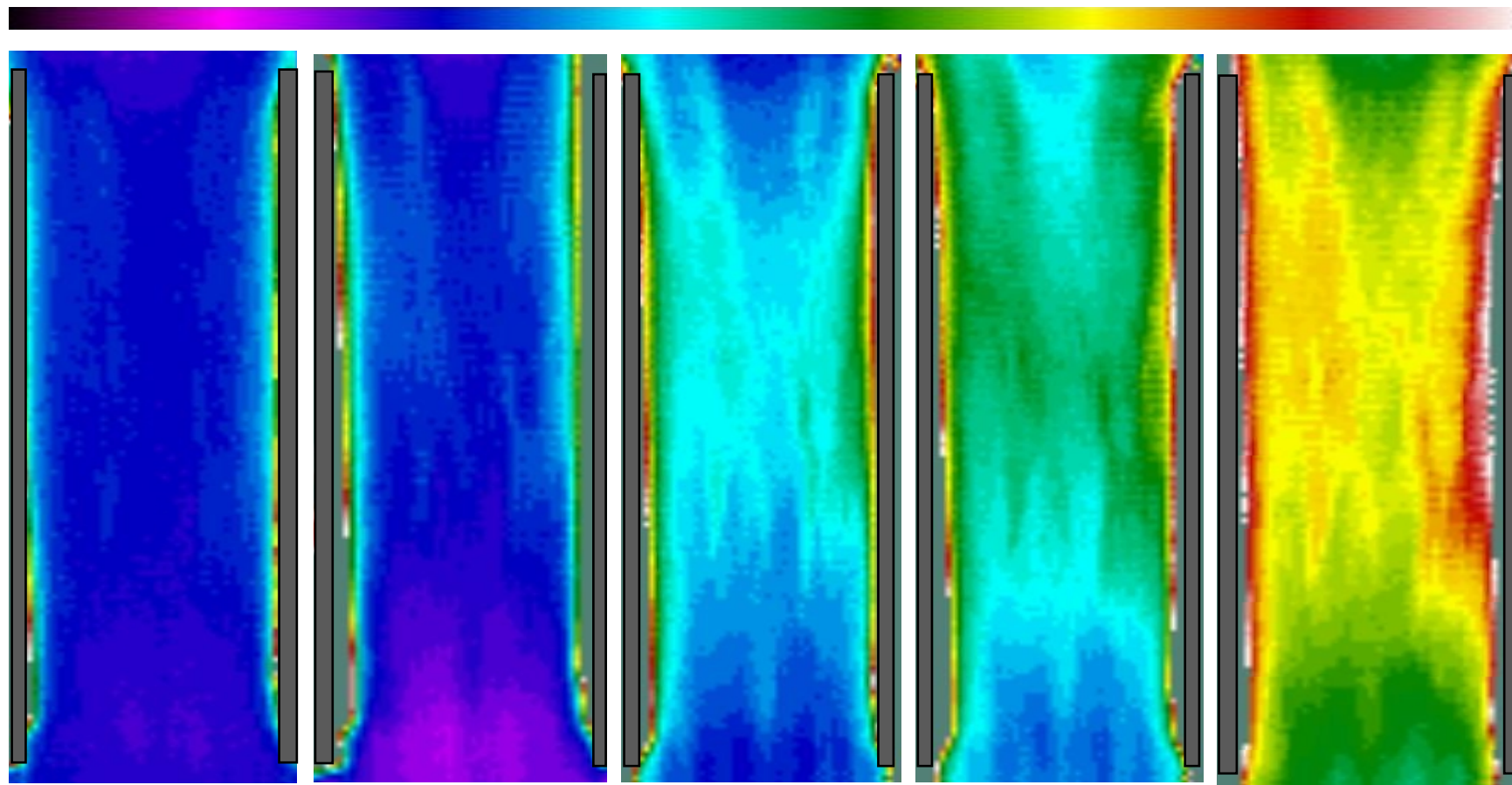
| $t_w = 40$ ºC | 50 ºC | 60 ºC | 70 ºC | 80 ºC |
| $t_\infty = 23.6$ ºC | 22.9 ºC | 24.0 ºC | 24.3 ºC | 24.9 ºC |

igure.6

emperature fields in the channel $s = 0.18$ m between the vertical isothermal heated plates as a function of their surface temperature t_w and the ambient temperature
, in the x, y, $z= 0.5$ B planes.

25.0   25.5   26.0   26.5   27.0   27.5   28.0   28.5   29.0   29.5   30.0 ºC

t_∞ =22.40 (*I*) / 25.00 (*II*) ºC

t_∞ =24.30 (*I*) / 26.10 (*II*) ºC

t_∞ =24.90 (*I*) / 27.30 (*II*) ºC

t_∞ =25.88 (*I*) / 26.88 (*II*) ºC

t_w =40 ºC t_w = 50 ºC t_w = 60 ºC t_w = 70 ºC
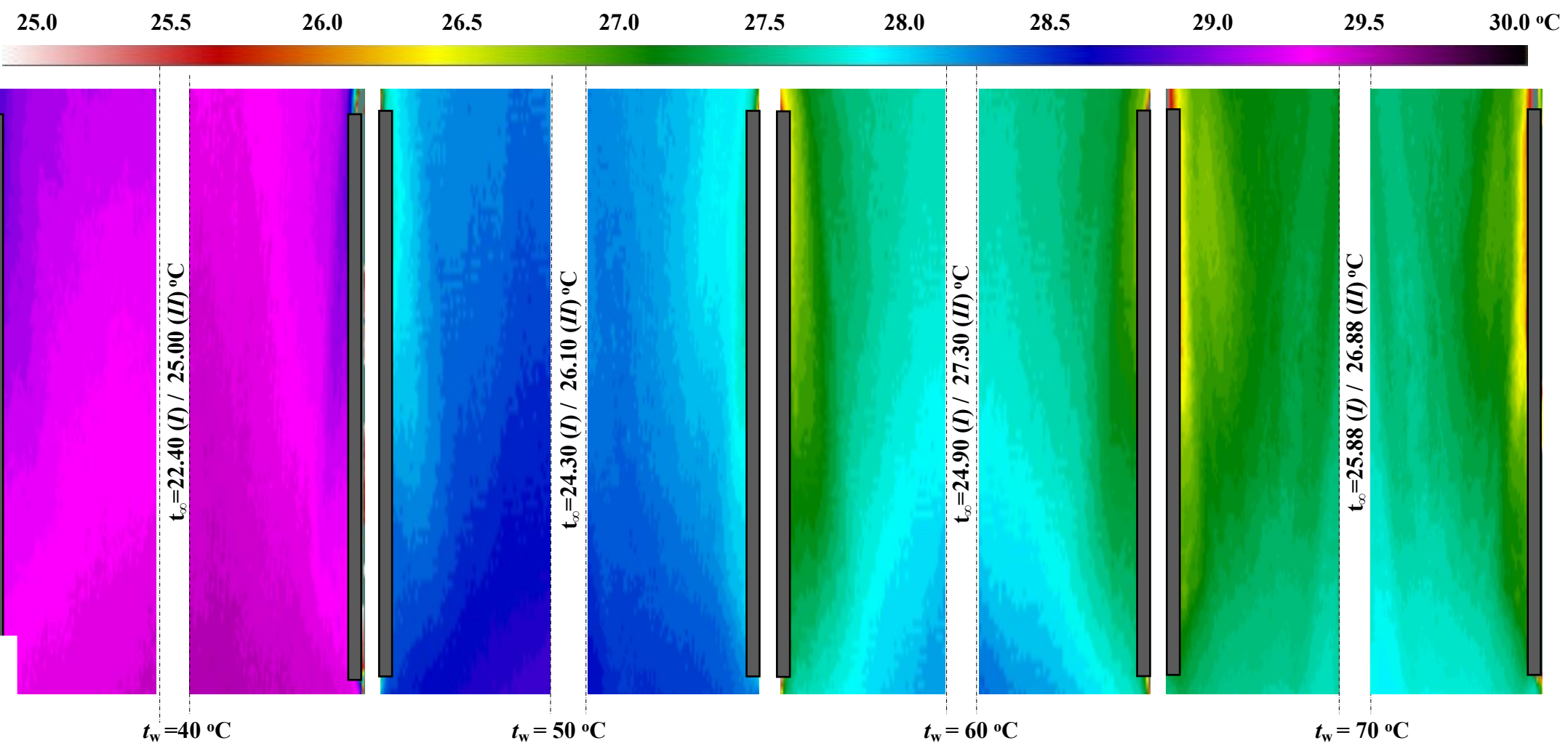
Figure 7

Temperature fields in the channel *s* = ∞ between two vertical isothermal heated plates as a function of their surface temperature t_w and the ambient temperature near plate *I* and *II* t_∞ in the *x*, *y*, *z*= 0.5 *B* planes.
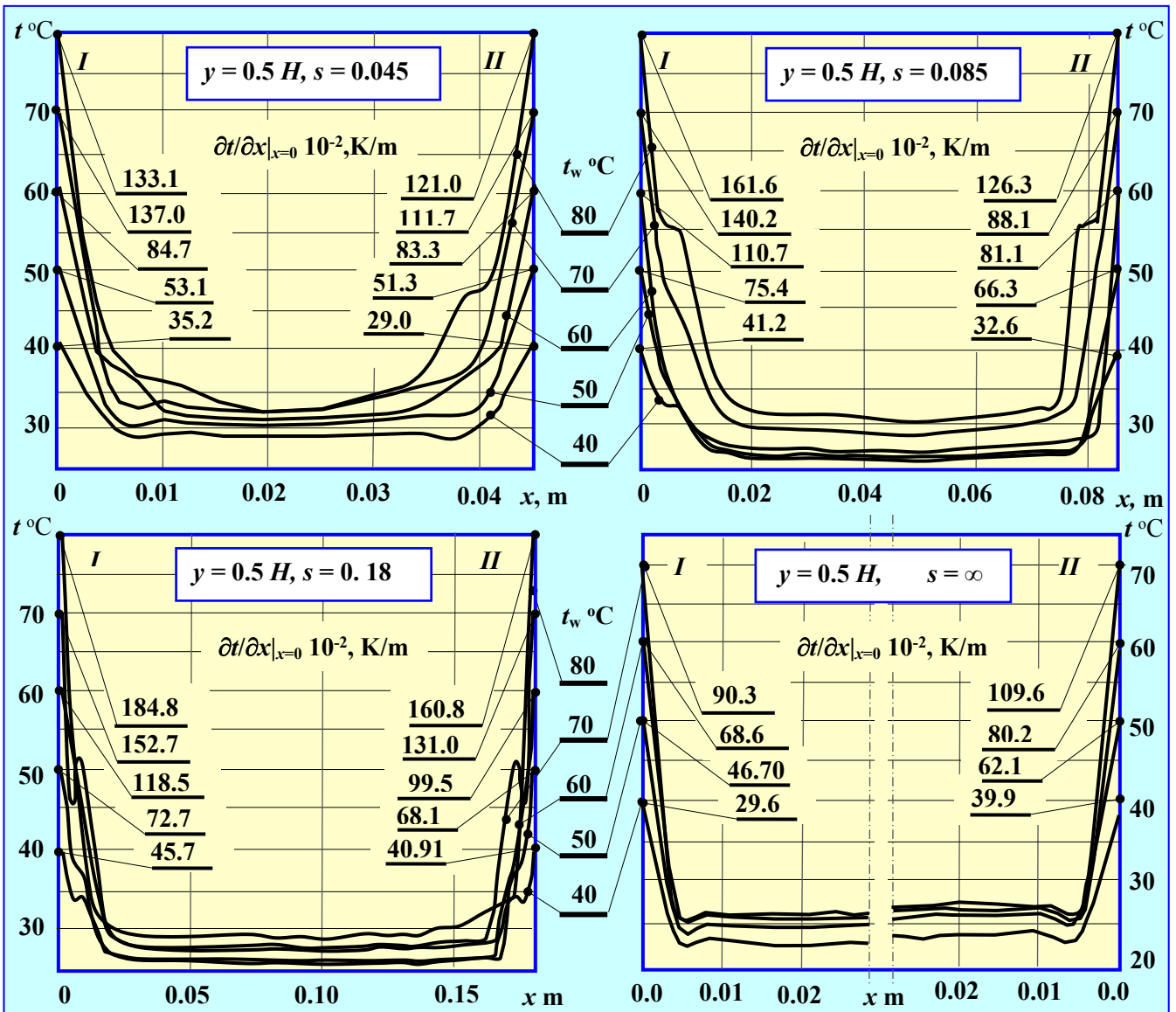
Figure 8

Temperature and temperature gradient distributions perpendicular to two vertical parallel heated surfaces that form three channels $s = 0.045$, 0.85, 0.18 m and ∞, measured at $y = 0.5\,H$ and $z = 0.5\,B$, as a function of temperature $t_w = 30, 40, 50, 60, 70$ and $80\ °C$ of the heated surfaces.
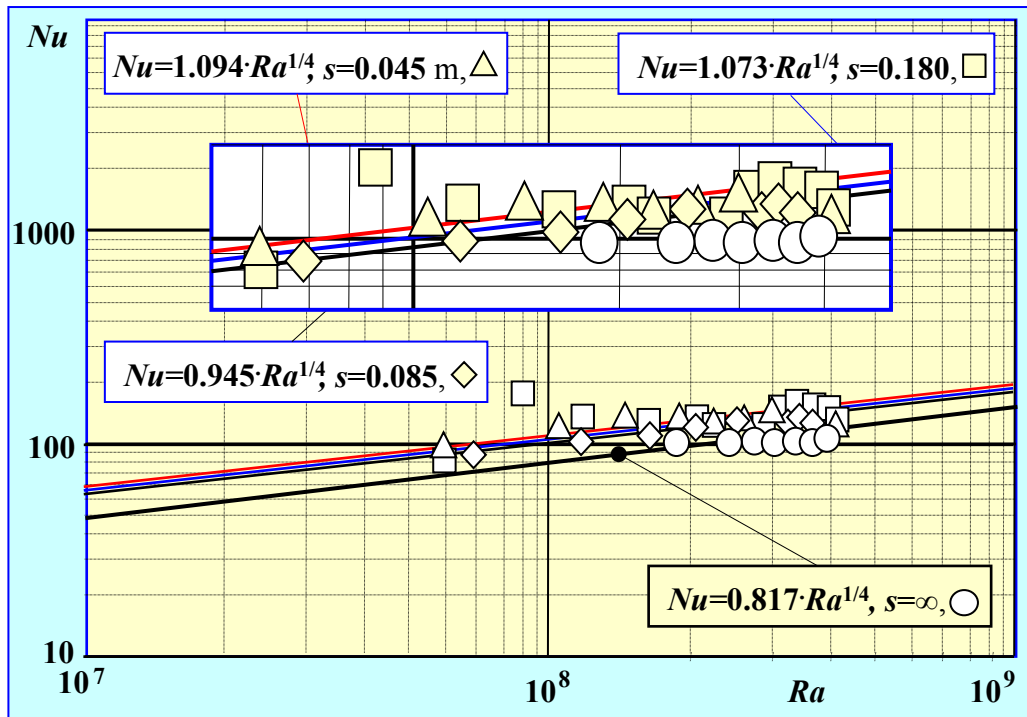
Figure 9

Convective heat transfer in open channels as a function of distance between isothermal vertical heated surfaces **s**, presented as Nusselt-Rayleigh relations with accuracy given by Eq 14 - 17. Size of experimental points (triangles, circles, squares and diamonds) corresponds with RMS (11.5 %).
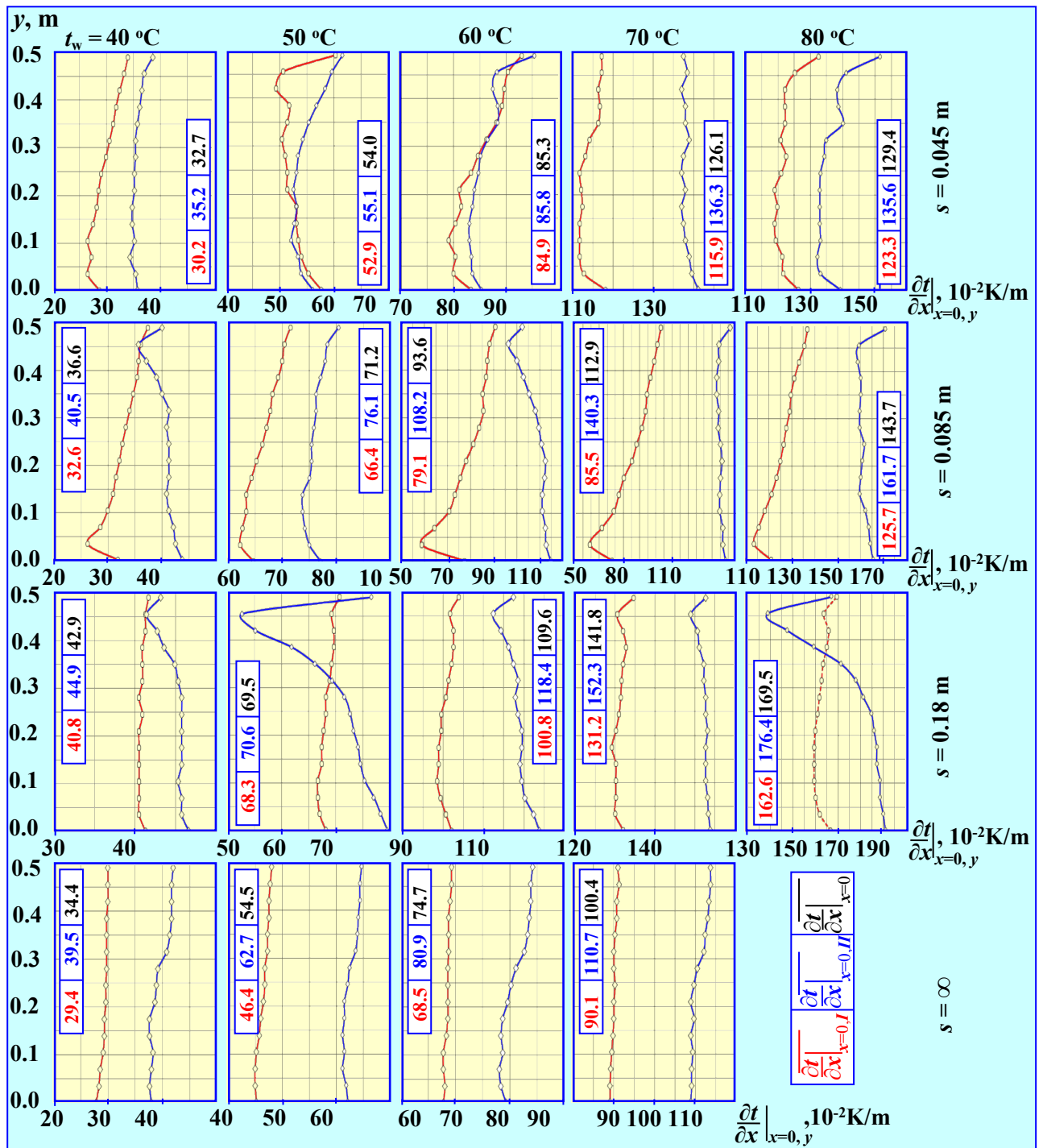
Figure 10

Distributions of temperature gradients in two heated surfaces (*I* - blue circles and *II* - red diamonds) and average values of these gradients for: I (red colour in frames) and II (blue colour) plates, as well as total for both surfaces (black colour), which form gaps *s* = 0.045, 085, 0.18 m and ∞ at the channel's half-width *z* = 0.5 *B*, as a function of temperature *t*$_w$ (constant for both heated surfaces). Accuracy of temperature gradients the same as in tab.3-6.
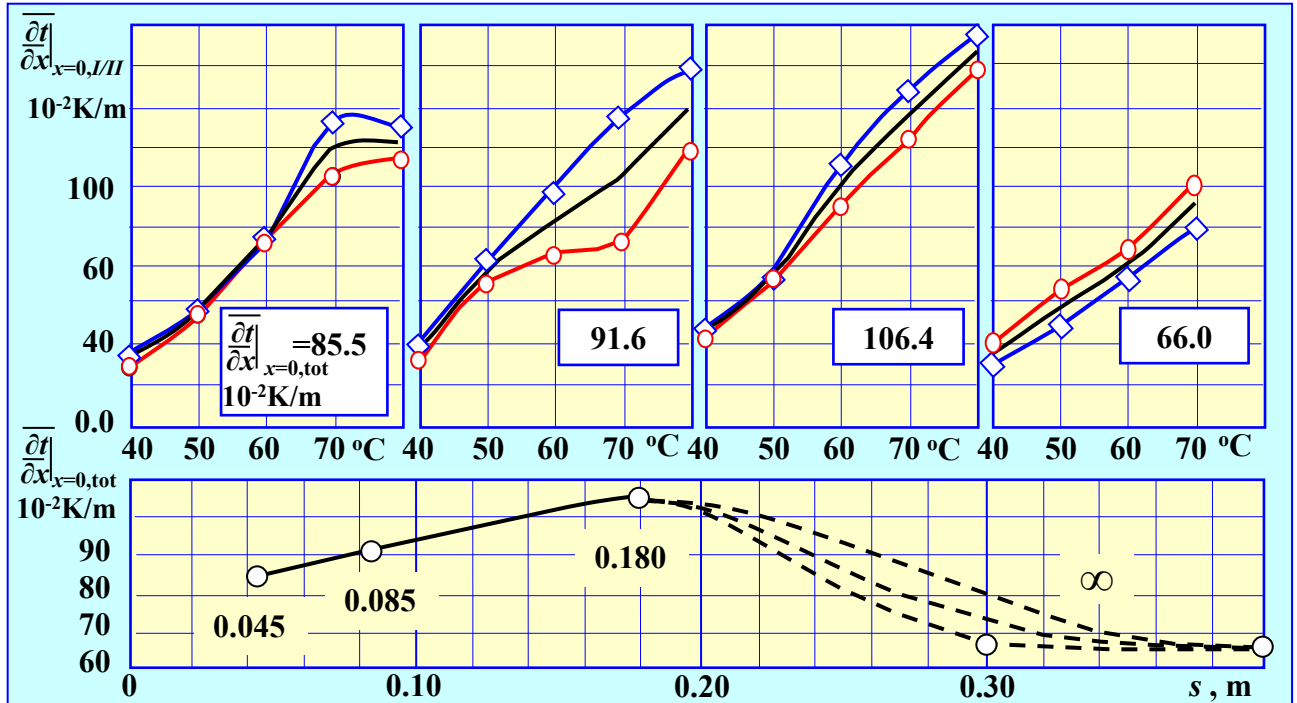
Figure 11

Graphical results of channel width effects on average wall temperature gradients (dt/dx|_{x=0}) for plates *I* (blue diamonds) and *II* (red circles) and for the whole channel.

Table 1. A summary of the most important research of natural convection in vertical, isothermal, symmetrically heated channels opened from four sides. Results of these studies allowed the formulation of the relations describing this phenomenon.

Author	Range of research	Obtained solution	Litera-ture
Elenbass	The first experimental and theoretical study (1942) of natural convective heat transfer in a vertical channel and in air.	$Nu_0 = \frac{Ra^*}{24} \cdot \left(1 - e^{-35/Ra^*}\right)^{3/4}$ with two asymptotes: $Nu_0\text{-}Nu_{bl}=0.60 Ra^{*1/4}$ for $Ra^* \to \infty$ $Nu_0\text{-}Nu_{fd}=0.333 Ra^{*1/4}$ for $Ra^* \to 0$	[31]
Raithby and Hollands, Aung, Fletcher and Sernas	Natural convection in vertical open channels. The authors modified Elebass' relation and divided it into two limiting cases: $s \to 0$ and $s \to \infty$.	$Nu_0 = \left(Nu_{fd}^m + Nu_{bl}^m\right)^{1/m}$; $m = -1.9$ where: $Nu_{fd} = Ra^*/24$, for $b \to 0$, $Nu_{bl} = 0.62 \cdot (Ra^*)^{1/4}$, for $b \to \infty$	[66], [67], [45]
Sparrow, Bahrami Ormiston Martin et. al.	Vertical open channels, experiment, -//- numerical solutions, -//- detailed analysis of the problem mentioned above	$\widetilde{Nu}_{fd} = \frac{\widetilde{Ra}}{6} \cdot \left(1 + \sqrt{1 + \frac{12}{\widetilde{Ra}}}\right)$ with two asymptotes $\widetilde{Nu}_{fd} = \sqrt{\frac{\widetilde{Ra}}{3}}$ for $\widetilde{Ra} \to 0$ and $\widetilde{Nu}_{fd} = \frac{\widetilde{Ra}}{3}$ for $\widetilde{Ra} \to \infty$	[20], [48], [49]
Churchill, Usagi	Vertical open channels with symmetrically heated, rectangular short plates, air and $10^4 < Ra < 10^9$	$Nu_0 = \left[\left(\frac{Ra^*}{24}\right)^{-m} + \left(0.59\sqrt[4]{Ra^*}\right)^{-n}\right]^{\frac{-1}{m}}$	[28]
Bar-Cohen et. al.	Optimizing the distance between heating plates in a multi-plate heater s_{opt} for an optimal value of the Nusselt number $Nu_{b,opt}$.	$Nu_0 = \left[\frac{576}{Ra^{*2}} + \frac{2.873}{\sqrt{Ra^*}}\right]^{-0.5}$ $s_{opt} = 2.714\, P^{-0.25}$ and $Nu_{b,opt} = 1.31$ where: $P = Ra/H^4$	[23] [24]

Table 2. Temperature distributions for the set temperatures of heated vertical plates t_w = 40, 50, 60, 70 and 80 °C within channels with different widths s between the plates on the (x, y, $z=0.5\,B$) plane, at the level $y= 0.5\,H$.

Plate *I*										Plate *II*
Plate spacing, $s = 0.045$ m										
	x_0	x_1	x_2	x_3		$x_i \approx x_{s/2}$	x_{n-3}	x_{n-2}	x_{n-1}	$x_n=s$
	$t_0=t_w$	t_1	t_2	t_3		$t_{\infty,y=H/2}$	t_{n-3}	t_{n-2}	t_{n-1}	$t_n= t_w$
$x \cdot 10^{-3}$, m	0	3.7	7.4	11.1	….	22.5	35.7	38.8	41.9	45
t, °C	40	29.3	28.9	28.6	….	28.5	28.5	28.7	29.1	40
$x \cdot 10^{-3}$, m	0	3.5	7.0	10.5	….	22.5	34.8	38.2	41.6	45
t, °C	50	31.3	30.5	30.0	….	30.0	30.5	31.3	32.7	50
$x \cdot 10^{-3}$, m	0	3.4	6.8	10.2	….	22.5	33.0	37.0	41.0	45
t, °C	60	31.9	31.2	30.7	….	30.63	31.0	31.5	32.6	60
$x \cdot 10^{-3}$, m	0	3.1	6.2	9.3	….	22.5	36.9	40.0	42.3	45
t, °C	70	35.2	33.9	33.4	….	32.1	31.3	32.0	33.0	70
$x \cdot 10^{-3}$, m	0	3.7	7.4	11.1	….	22.5	35.4	38.6	41.8	45
t, °C	80	35.4	33.4	32.3	….	32.0	32.6	34.2	37.0	80
Plate spacing, $s = 0.085$ m										
$x \cdot 10^{-3}$, m	0	3.7	7.4	11.1	….		76.0	79.0	82.0	85
t, °C	40	28.0	27.4	27.2	….	26.6	26.9	27.1	27.6	40
$x \cdot 10^{-3}$, m	0	3.4	6.8	10.2	….		76.0	79.0	82.0	85
t, °C	50	27.6	27.1	26.9	….	26.2	26.5	26.6	27.5	50
$x \cdot 10^{-3}$, m	0	3.7	7.4	11.1	….		76.6	79.4	82.2	85
t, °C	60	30.1	28.9	28.4	….	27.4	27.7	28.2	29.0	60
$x \cdot 10^{-3}$, m	0	4.1	8.2	12.3	….		76.6	79.4	82.2	85
t, °C	70	34.3	31.9	31.1	….	29.3	30.1	30.1	30.7	70
$x \cdot 10^{-3}$, m	0	3.7	7.4	11.1	….		76.3	79.2	82.1	85
t, °C	80	33.5	32.9	32.2	….	31.3	31.9	32.2	33.2	80
Plate spacing, $s = 0.18$ m										

x·10⁻³, m / t, °C										
x·10⁻³, m	0	3.2	6.4	9.6	....		....	171.3	174.2	177.1	180
t, °C	40	26.7	26.6	26.6	....	26.2	....	26.5	26.6	26.7	40
x·10⁻³, m	0	3.4	6.8	10.2	....		....	171.0	174.0	177.0	180
t, °C	50	27.0	26.6	26.4	....	26.0	....	26.7	27.2	28.2	50
x·10⁻³, m	0	3.1	6.2	9.3	....		....	171.6	174.4	177.2	180
t, °C	60	29.0	28.4	28.3	....	27.6	....	28.0	28.2	28.9	60
x·10⁻³, m	0	3.1	6.2	9.3	....		....	171.9	174.6	177.3	180
t, °C	70	29.2	28.7	28.6	....	28.1	....	28.1	28.3	28.6	70
x·10⁻³, m	0	3.0	6.0	9.0	....		....	157.2	164.8	172.4	180
t, °C	80	31.7	31.0	30.5	....	29.3	....	29.3	29.3	29.4	80

Plate I				Plate spacing, s = ∞						Plate II
x·10⁻³, m	0	4.1	8.1	12.2	....	∞	....	-14.7	-9.8	-4.9	0
t, °C	40	24.2	23.5	23.2	....	22.4/25.0	....	25.3	25.3	25.5	40
x·10⁻³, m	0	3.9	7.8	11.7	....	∞	....	-14.7	-9.8	-4.9	0
t, °C	50	25.7	25.4	25.2	....	24.3/26.1	....	26.7	26.9	27.1	50
x·10⁻³, m	0	4.1	8.2	12.3	....	∞	....	-13.8	-9.2	-4.6	0
t, °C	60	27.1	26.6	26.1	....	24.9/27.3	....	28.2	28.3	28.5	60
x·10⁻³, m	0	3.9	7.8	11.7	....	∞	....	-13.8	-9.2	-4.6	0
t, °C	70	28.2	27.7	27.5	....	25.9/26.9	....	28.3	28.3	28.5	70
Accuracy of temperature measurement Δt =±0.1										

Table 3. Temperature gradient distributions along vertical plates *I* and *II* for constant surface temperature t_w = 40, 50, 60, 70, and 80 °C within the channel and for the width between the heated plates *s* = 0.045 m.

$y \cdot 10^{-2}$, m	(I) $\partial t/\partial x \big|_{x=0,y} 10^{-2}$ / (II) $\partial t/\partial x \big|_{x=0,y} \cdot 10^{-2}$, K/m				
	t_w, °C 40	50	60	70	80
	t_∞, °C 25.3±0.1	25.3±0.1	25±0.1	24.9±0.1	25.1±0.1
0.0	35.7 / 28.7	56.1 / 57.6	85.3 / 83.3	141.2 / 118.2	139.3 / 126.3
3.5	35.4 / 26.5	53.9 / 55.2	83.6 / 80.0	139.6 / 112.7	133.1 / 121.7
7.0	34.4 / 27.2	53.4 / 53.9	83.4 / 80.4	138. 9 / 111.7	132.1/ 121.4
10.5	35.2 / 26.5	52.2 / 53.4	83.0 / 79.1	138.0 / 111.7	133.1 / 119.3
14.0	27.5 / 34.7	53.0 / 52.7	80.4 / 83.0	111.7 / 137.5	119.0 / 132.9
17.5	34.7 / 28.2	53.1 / 53.0	83.6 / 81.5	137.0 / 112.3	132.9 / 119.8
21.0	35.2 / 28.5	52.5 / 51.3	83.9 / 81.1	138.0 / 112.1	132.9 /119.0
24.5 (0.5 H)	35.2 / 29.0	53.1 / 51.3	84.7 / 83.3	137.0 / 111.7	133.1 / 121.0
28.0	35.4 / 29.9	53.4 / 50.9	85.1 / 84.6	137.5 / 113.1	134.2 / 122.5
31.5	35.4 / 30. 6	54.3 / 50.4	86.5 / 86.3	138.9 / 114.1	134.8 / 120.9
35.0	35.7 / 31.2	55.4 / 51.3	88.4 / 88.1	138.0 / 116.4	140.1 / 122.2
38.5	36.2 / 31.7	56.8 / 51.7	88.4 / 89.2	138.0 / 116.7	138.7 / 122.2
42.0	36.5 / 32.4	58.4 / 49.3	87.4 / 89.6	137.0 /116.4	138.3 / 122.2
45.5	37.0 / 33.3	59.6 / 50.6	88.2 / 90.4	138.4 / 117.2	141.0 / 125.3
49.0 (H)	38.6 / 33.9	61.6 / 60.3	95.4 / 92.9	137.5 / 117.2	151.5 / 132.6
Average *I/II*	**35.2 / 30.2**	**55.1 / 52.9**	**85.8 / 84.9**	**136.3 / 115.9**	**135.6 / 123.3**
Channel	**32.7±1.9**	**54.0±3.1**	**85.3±4.9**	**126.1±7.2**	**129.4±7.4**

Table 4. Temperature gradient distributions along vertical plates *I* and *II* for constant surface temperature t_w = 40, 50, 60, 70 and 80 °C within the channel and for the width between the plates *s* = 0.085 m.

$y \cdot 10^{-2}$, m	(*I*) $\partial t/\partial x \big|_{x=0,y}$ 10^{-2} / (*II*) $\partial t/\partial x \big|_{x=0,y} \cdot 10^{-2}$, K/m				
	t_w, °C 40	50	60	70	80
	t_∞, °C 23.0±0.1	23.5±0.1	23.4±0.1	24.3±0.1	26.2±0.1
0.0	43.7 / 31.7	77.1 / 64.6	114.7 / 77.4	143.3 / 73.1	165.5 / 120.7
3.5	42.5 / 26.1	75.0 / 62.2	112.7 / 58.7	141.5 / 59.3	164.2 / 113.4
7.0	42.1 / 28.5	74.2 / 62.6	112.5 / 64.3	141.5 / 66.5	163.5 / 115.4
10.5	41.2 / 29.9	73.7 / 63.3	111.1 / 70.6	139.7 / 74.1	162.0 /118.1
14.0	40.8 / 30.9	73.7 / 63.3	111.1 / 73.8	139.7 / 77.2	159.7 / 121.0
17.5	41.2/ 31.4	75.0 / 64.3	112.0 / 75.5	140.2 / 80.2	160.1 / 123.2
21.0	41.2 / 32.1	75.4 / 65.2	112.5 / 77.9	141.1 / 85.2	160.7 / 124.9
24.5 (0.5 H)	41.2 / 32.6	75.4 / 66.3	110.7 / 81.1	140.2 / 88.1	161.6 / 126.3
28.0	40.8 / 33.3	75.8 / 67.0	109.6 / 83.7	138.6 / 91.4	159.7 / 127.5
31.5	41.2 / 33.9	76.2 / 67.8	108.0 / 85.6	139.1 / 93.7	159.7 / 129.0
35.0	40.0 / 34.6	76.2 / 68.1	105.4 / 85.2	137.7 / 94.4	160.1 / 129.5
38.5	39.0 / 35.3	77.1 / 69.2	102.9 / 86.7	137.7 / 96.6	160.1 / 131.0
42.0	37.1 / 35.6	77.9 / 70.0	100.0 / 87.2	139.1 / 99.1	158.8 / 133.1
45.5	35.6 / 36.0	78.3 / 70.4	96.4 / 88.3	139.3 / 101.1	159.2 / 135.4
49.0 (H)	40.0 / 37.4	80.4 / 71.5	102.5 / 90.6	146.2 / 103.2	170.9 / 136.8
Average *I*/*II*	**40.5 / 32.6**	**76.1 / 66.4**	**108.2 / 79.1**	**140.3 / 85.5**	**161.7 / 125.7**
Channel	**36.6±2.1**	**71.2±4.1**	**93.6±5.3**	**112.9±6.4**	**143.7±8.2**

Table 5. Temperature gradient distributions along vertical plates *I* and *II* for constant surface temperature t_w = 40, 50, 60, 70 and 80 °C within the channel and for the width between the plates *s* = 0.180 m.

$y \cdot 10^{-2}$, m	(*I*) $\partial t/\partial x \big|_{x=0,y}$ 10^{-2} / (*II*) $\partial t/\partial x \big|_{x=0,y} \cdot 10^{-2}$, K/m				
	t_w, °C 40	50	60	70	80
	t_∞, °C 23.6±0.1	22.9±0.1	24±0.1	24.3±0.1	24.9±0.1
0.0	46.6 / 41.3	79.6 /68.1	123.8 / 102.1	153.9 / 132.0	190.9 / 166.7
3.5	45.7/ 40.5	78.3 / 67.0	122.4 / 100.7	153.4 / 130.0	190.0 / 161.9
7.0	45.7 / 40.5	77.1 / 66.7	120.2 / 99.3	153.1 / 130.2	188.6 / 160.0
10.5	45.3 / 40.5	75.4 / 66.7	119.5 / 98.5	152.7 / 130.2	188.6 / 159.4
14.0	45.7/ 40.5	74.6 / 67.4	119.0 / 98.9	152.7 / 130.2	187.1 / 159.4
17.5	45.7 / 40.5	74.2 / 67.4	119.5 / 98.9	152.7 / 129.2	187.1 / 159.4
21.0	45.7 / 40.5	73.3 / 67.8	119.5 / 99.5	153.1 / 130.2	185.9 / 159.8
24.5 (0.5 H)	45.7 / 40.9	72.7 / 68.1	118.5 / 99.5	152.7 / 131.0	184.8 / 160.8
28.0	45.7 / 40.5	71.7 / 68.1	117.9 / 100.7	152.7 / 131.4	181.2 / 161.7
31.5	45.3 / 40.9	69.4 / 68.9	118.5 / 101.3	152.2 / 131.6	177.9 / 162.7
35.0	44.9 / 40.9	66.2 / 69.2	117.4 / 102.1	152.2 / 132.0	171.2 / 163.3
38.5	43.6 / 40.9	61.9 / 69.6	116.2 / 102.5	151.1 / 132.8	159.3 / 165.0
42.0	42.7 / 41.3	55.2 / 69.6	114.3 / 102.5	150.6 / 132.0	147.4 / 165.8
45.5	41.4 / 41.3	52.7 / 69.2	112.4 / 101.7	149.0 / 130.6	138.8 / 163.7
49.0 (H)	43.1 / 41.7	76.7 / 70.7	117.4 / 103.9	152.7 / 134.6	166.9 / 169.4

Average *I/ II*	**44.9 / 40.8**	**70.6 / 68.3**	**118.4 / 100.8**	**152.3 / 131.2**	**176.4 / 162.6**
Channel	**42.9±2.4**	**69.5±4.0**	**109.6±6.2**	**141.8±8.1**	**169.5±9.7**

Table 6. Temperature gradient distributions along vertical plates I and II for a constant surface temperature t_w = 40, 45, 50, 60, and 70 °C within the channel and for the width between the plates $s = \infty$ m.

$y \cdot 10^{-2}$, m	(I) $\partial t/\partial x \big|_{x=0,y} \cdot 10^{-2}$ / (II) $\partial t/\partial x \big|_{x=0,y} \cdot 10^{-2}$, K/m			
	t_w, °C 40	50	60	70
	t_∞, °C (*I*) 23.1±0.1	24.5±0.1	25.3±0.1	25.1±0.1
	t_∞, °C (*II*) 20.5±0.1	21.5±0.1	22.4±0.1	23.5±0.1
0.0	27.8 / 37.9	45.1 / 62.1	67.7 / 79.3	89.1 / 108.8
3.5	28.3 / 37.6	44.9 / 61.8	68.0 / 78.3	89.1 / 109.0
7.0	28.6 / 37.9	44.9 / 61.1	67.7 / 78.0	89.2 / 109.0
10.5	29.1 / 38.3	45.1 / 61.5	67.7 / 78.7	89.5 / 109.3
14.0	29.3 / 37.6	45.6 / 61.1	68.3 / 78.3	89.8 / 108.8
17.5	29.3 / 37.6	45.9 / 61.5	68.6 / 78.7	90.1 / 109.6
21.0	29.6 / 38.6	46.4 / 61.5	68.6 / 79.6	90.1 / 108.8
24.5 (0.5 H)	29.6 / 38.9	46.7 / 62.1	68.6 / 80.2	90.3 / 109.6
28.0	29.7 / 39.2	46.7 / 62.4	68.6 / 81.1	90.1 / 110.4
31.5	29.7 / 40.7	47.2 / 63.5	68.7 / 82.6	90.1 / 112.0
35.0	29.7 / 41.4	47.2 / 63.9	68.7 / 83.2	90.3 / 112.3
38.5	29.7 / 41.6	47.4 / 64.0	68.7 / 83.5	90.7 / 113.0
42.0	30.0 / 41.6	47.4 / 64.3	69.0 / 83.8	90.7 / 113.3
45.5	30.0 / 41.6	47.7 / 64.3	69.2 / 83.8	91.3 / 113.6
49.0 (H)	30.0 / 42.0	48.0 / 64.7	69.2 / 84.1	91.0 / 113.6
Average *I/II*	**29.4 / 39.5**	**46.4 / 62.7**	**68.5 / 80.9**	**90.1 / 110.7**
Channel	**34.4±2.0**	**54.5±3.1**	**74.7±4.3**	**100.4±5.7**

Table 7. Comparison results of convective heat transfer in channels with different *s*, obtained using balance and gradient methods, and the differences between them.

s, m	$Nu_b/Ra^{1/4}$, -	$Nu/Ra^{1/4}$, -	Difference, %
0.045	0.491 Eq.(4)	1.094 Eq.(14)	45
0.085	0.480 Eq.(5)	0.945 Eq.(15)	50
0.180	0.497 Eq.(6)	1.073 Eq.(16)	46
∞	0.486 Eq.(7)	0.817 Eq.(17)	59